Published in final edited form as:
Hepatology. 2009 August ; 50(2): 443–452. doi:10.1002/hep.23033.

Impaired Liver Regeneration in Mice Lacking Glycine *N*-Methyltransferase

Marta Varela-Rey[1,†], **David Fernández-Ramos**[1,†], **Nuria Martínez-López**[1], **Nieves Embade**[1], **Laura Gómez-Santos**[1], **Naiara Beraza**[1,†], **Mercedes Vázquez-Chantada**[1], **Juan Rodríguez**[1], **Zigmund Luka**[2], **Conrad Wagner**[2,3], **Shelly C Lu**[4], **M Luz Martínez-Chantar**[1], and **José M Mato**[1]

[1]CIC bioGUNE, Centro de Investigación Biomédica en Red de Enfermedades Hepáticas y Digestivas (Ciberedh), Technology Park of Bizkaia, 48160-Derio, Bizkaia, Spain.

[2]Department of Biochemistry, Vanderbilt University, Nashville, TN 37232-0146.

[3]Tennessee Valley Department of Medical Affairs Medical Center, Nashville, TN 37212.

[4]Division of Gastrointestinal and Liver Diseases, USC Research Center for Liver Diseases, Southern California Research Center for Alcoholic Liver and Pancreatic Diseases and Cirrhosis, Keck School of Medicine, University of Southern California, Los Angeles, CA 90033

Abstract

Hepatic S-adenosylmethionine (SAMe) is maintained constant by the action of methionine adenosyltransferase I/III (MATI/III), that converts methionine into SAMe, and glycine *N*-methyltransferase (GNMT), that eliminates excess SAMe to avoid aberrant methylation reactions. During liver regeneration after partial hepatectomy (PH) MATI/III activity is inhibited leading to a decrease in SAMe. This injury-related reduction in SAMe promotes hepatocyte proliferation because SAMe inhibits hepatocyte DNA synthesis. In MATI/III deficient mice, hepatic SAMe is reduced resulting in uncontrolled hepatocyte growth and impaired liver regeneration. These observations suggest that a reduction in SAMe is crucial for successful liver regeneration. In support of this hypothesis we report that liver regeneration is impaired in GNMT knockout (GNMT-KO) mice. Liver SAMe is 50-fold higher in GNMT-KO mice that in control animals and is maintained constant following PH. Mortality after PH was higher in GNMT-KO mice than in control animals. In GNMT-KO mice, nuclear factor κB (NFκB), signal transducer and activator of transcription-3 (STAT3), inducible nitric oxide synthase (iNOS), cyclin D1, cyclin A and poly (ADP-ribose) polymerase were activated at baseline. PH in GNMT-KO mice was followed by the inactivation of STAT3 phosphorylation and iNOS expression. NFκB, cyclin D1 and cyclin A were not further activated after PH. The LKB1/AMP-activated protein kinase/endothelial nitric oxide synthase cascade was inhibited, and cytoplasmic HuR translocation was blocked despite preserved induction of DNA synthesis in GNMT-KO after PH. Furthermore, a previously unexpected relationship between AMPK phosphorylation and NFκB activation was uncovered.

Conclusions—These results indicate that multiple signaling pathways are impaired during the liver regenerative response in GNMT-KO mice, suggesting that GNMT plays a critical role during liver regeneration promoting hepatocyte viability and normal proliferation.

Contact information Corresponding author: José M Mato, CIC bioGUNE, Technology Park of Bizkaia, 48160 Derio, Bizkaia, Spain. director@cicbiogune.es; **Tel**: 944-061300; **Fax**: 944-061301.
MVR and DF contributed equally to this paper.
[†]Contributed equally to this paper. MLMC and JMM share senior authorship.

Keywords

LKB1/AMPK/eNOS cascade; S-adenosylmethionine; hepatocyte growth factor; HuR; NFκB

INTRODUCTION

Methionine is an essential amino acid metabolized mainly by the liver where it is first converted to S-adenosylmethionine (SAMe), through a reaction catalyzed by the enzyme methionine adenosyltransferase I/III (MATI/III), and then to S-adenosylhomocysteine, by the action of the enzyme glycine *N*-methyltransferase (GNMT) (1). MATI and MATIII are expressed mainly in the adult liver. They are, respectively, tetramers and dimmers of the same single subunit encoded by the gene MAT1A (2). A third isoenzyme, MATII, contains a catalytic subunit encoded by a second gene, MAT2A, and is expressed in all tissues including adult liver (2). MAT1A knockout (MAT1A-KO) mice have elevated plasma levels of methionine and reduced hepatic SAMe content (3), indicating that MATII cannot compensate for the loss of MATI/III. Although there are many enzymes that utilize SAMe in the liver, quantitatively the most important is GNMT (1). Mice lacking functional GNMT (GNMT-KO), a gene mainly expressed in the liver, have a 50-fold increase in hepatic SAMe content (4,5) indicating that the hepatic reduction in total transmethylation flux caused by the absence of GNMT cannot be compensated by other methyltransferases that are abundant in the liver, such as phosphatidyl *N*-methyltransferase and guanidinoacetate *N*-methyltransferase. Accordingly, disruption of phosphatidyl *N*-methyltransferase or guanidinoacetate *N*-methyltransferase in mice has little or no effect on hepatic SAMe content (1). These results demonstrate that hepatic SAMe content is regulated by the combined action of MATI/III and GNMT.

Accumulating evidence indicates that SAMe is a critical regulator of hepatocyte growth (6). Whereas chronic hepatic SAMe deficiency in MAT1A-KO mice leads to uncontrolled hepatocyte growth and malignant degeneration (7), a fall in hepatic SAMe levels precedes liver regeneration after 2/3 partial hepatectomy (PH) and is necessary for normal regeneration to occur (8). The mechanism involves the ability of SAMe to inhibit the mitogenic effect of hepatocyte growth factor (HGF), which was demonstrated using cultured rat and mouse hepatocytes (9,10). SAMe blocks HGF-induced hepatocyte proliferation by inhibiting the phosphorylation and activation of an LKB1/AMP-actiavted protein kinase (AMPK)/endothelial nitric oxide synthase (eNOS) cascade, a novel pathway that is downstream the HGF/MET receptor but is distinct from the Ras/ERK/MAPK pathway (10,11). This pathway is activated in mice during liver regeneration after PH and its down-regulation, using interference RNA, leads to the inhibition of HGF-induced DNA synthesis in hepatocytes (11). The LKB1/AMPK/eNOS cascade is constitutively activated in MAT1A-KO mice (10,11), which agrees with the observation that these animals have a chronic reduction in hepatic SAMe content, increased hepatocyte DNA synthesis and spontaneously develop hepatocellular carcinoma (HCC) (3,7). Conversely, SAMe treatment before PH prevents the phosphorylation of the LKB1/AMPK/eNOS cascade and inhibits hepatocyte DNA synthesis (11). Here we analyzed, whether the excess of hepatic SAMe in GNMT-KO mice will inhibit the phosphorylation of the LKB1/AMPK/eNOS cascade after PH and if this will result in an impaired regenerative response of the liver. Furthermore, we analyzed if priming, that is the transition of the quiescent hepatocytes into the cell cycle after PH (12,13), is impaired in GNMT-KO mice and if the LKB1/AMPK/eNOS cascade is involved also in this process.

EXPERIMENTAL PROCEDURES

Partial Hepatectomy Experiments

Two-third PH was performed in 3-month-old male WT and GNMT-KO mice. Mice were fed a standard diet (Harland Teklad irradiated mouse diet 2014, Madison, WI) and housed in a temperature-controlled animal facility with 12 hours light-dark cycles. Animals were treated humanely, and all procedures were in compliance with our institutions' guidelines for the use of laboratory animals. PH was done according to the method of Higgins and Andersen (14) between 8 and 11 a.m., liver specimens removed (time zero) and snap frozen in liquid nitrogen or formalin fixed for subsequent analysis as described below. Groups of animals (n = 4 to 8) were sacrificed at 0.5, 6, 24 and 48-hours. Two hours before sacrifice, mice were injected i.p. with bromodeoxyuridine (BrdU, 100 mg/kg body weight) to assess hepatocyte DNA synthesis. At the time of sacrifice, livers were rapidly split into several pieces, some were snap frozen for subsequent RNA or protein extraction; others were formalin fixed for histology and immunohistochemistry as described below.

BrdU Immunohistochemistry

Frozen liver tissue sections were fixed with acetone for 1 min at room temperature followed by treatment with 2 M HCl at 37°C for 20 min. The sections were then neutralized with 0.1 M sodium borate for 10 min and mouse monoclonal anti-BrdU antibody (Roche Diagnostics, UK) applied overnight at 4°C followed by goat anti-mouse Rhodamine antibody (Cappel, PA, USA) and Hoescht nuclear dye. The number of BrdU positive cells was counted and expressed as the number of positive cells per field, as visualized by Hoescht labeling.

Proliferating Cell Nuclear Antigen (PCNA) Immunohistochemistry

Sections from formalin-fixed and paraffin-embedded liver tissue were stained with mouse monoclonal anti-PCNA primary antibody (Santa Cruz Biotechnology), followed by peroxidase-labeled goat antimouse antibody (Dako Envision System) at room temperature for 3 hours, stained with the peroxidase substrate 3,3 2-diamino-bencidine chromogen (Dako) and counterstained with haematoxylin.

Isolation and Culture of Hepatocytes

Hepatocytes were isolated from 3-month-old male WT mice, by collagenase perfusion (Gibco-BRL) as described previously (15). Viable cells were purified by centrifugation in Percoll gradient. Viability of the cells, as judged by the trypan blue exclusion test, was more than 85%. Isolated hepatocytes were seeded over collagen coated 60 mm tissue culture dishes at a density of 7.600 cells/mm^2 in minimum essential medium (MEM) supplemented with 10% bovine fetal serum, and placed in a 5% CO_2-95 % air incubator, at 37 °C. After 2 hours of attachment, the culture medium was removed and replaced by serum free MEM. After plating for 4 hours, hepatocytes were incubated for 2 hours with 40 μM Compound C (CC), an inhibitor of AMPK phosphorylation (16), and then treated with human recombinant tumor necrosis factor α (TNF-α RD systems, 10 ng/ml).

RNA isolation and real-time PCR

Total RNA was isolated using RNeasy Mini Kit (Qiagen), including DNase treatment on column. 1.5 μg of total RNA were retrotranscribed with Super Script III (Invitrogen) in the presence of random primers and oligo dT following manufacturer's instructions. Real time PCR was performed using BioRad iCycler thermalcycler. 5 μl of a 1/20 dilution were used in each PCR reaction in a total reaction volume of 30 μl using iQ SYBR Green Super Mix (BioRad) and all reactions were performed in duplicates. PCR was executed with the

following primers: iNOSF 5'-GGCAGCCTGTGAGACCTTTG -3', iNOSR 5'-GCATTGGAAGTGAAGCGTTTC-3'; ARPF 5'-CGACCTGGAAAGTCCAACTAC -3', ARPR 5'-ATCTGCTGCATCTGCTTG -3'. After checking specificity of the PCR products with the melting curve, Ct values were extrapolated to a standard curve performed simultaneously with the samples and data was then normalized to ARP expression.

Total, cytosolic and nuclear protein isolation

Frozen liver tissue samples (50 mg) were homogenized in 1 ml of lysis buffer (10 mM Tris/HCl pH 7.6. 5 mM EDTA, 50 mM NaCl, 1% Triton X–100, complete protease inhibitor cocktail, and 50 mM NaF). Samples were centrifuged (15.000 g, 1 hour, 4°C) and supernatants collected. Cytosolic and nuclear fractions from frozen liver samples and cultured hepatocytes were prepared as described in the subcellular proteome extraction kit from Calbiochem.

Immunoblot analysis

Samples were separated by SDS-PAGE and analyzed by immunoblotting using commercial antibodies. Blots were developed with a secondary anti-rabbit or anti-mouse antibody conjugated to horseradish peroxidase (Invitrogen, Carlsbad, CA) and the luminal-chemiluminescence reagent (ECL, Amersham Biosciences, Uppsala). The processed blots were exposed to X-ray film, and the autoradiograms analyzed. Commercial antibodies used are: LKB1, GAPDH and Lamin A from AbCAM; AMPKα1 from Upstate; eNOS from BD Transduction Laboratories; cyclin D1, cyclin E, cyclin A, p27, and HuR from Santa Cruz Biotechnology; PARP, STAT3, P-Tyr(705) STAT3, P-Ser(536) p65, p65, P-Ser(32) IκBα, IκBα, P-Ser(429) LKB1, P-Thr(172) AMIIKα1 and P-Ser(1177) eNOS from Cell Signalling Technology; and β-actin from SIGMA.

SAMe measurement

Hepatic SAMe was determined by LC/MS using a Waters ACQUITY-UPLC system coupled to a Waters Micromass LCT Premier Mass Spectrometer equipped with a Lockspray ionization source as described previously (11).

Statistical analysis

Student *t* test and Kruskal-Wallis test were used to evaluate statistical significance. Values of $p < 0.05$ were considered statistically significant.

RESULTS

Increased mortality in GNMT knockout mice during liver regeneration after PH

Three-month-old male GNMT-KO mice and age-matched WT animals were subjected to PH. Mortality during the first 48 hr after PH was higher in the GNMT-KO mice (38%) than in control animals (0%) (Fig.1a). Hepatic apoptosis, as evidenced by poly (ADP-ribose) polymerase (PARP) protein cleavage, was also markedly increased in GNMT-KO mice before PH and remained elevated in all surviving GNMT-KO mice (Fig.1b). Liver regeneration was assessed in the knockout and WT mice by using PCNA staining and BrdU incorporation. PCNA is an auxiliary protein of DNA polymerase delta. Its expression is cell cycle dependent, being detected in late G_1 and remains increased throughout the S phase and into the early post-replicative G_2 period (17). BrdU is a thymidine analog that is incorporated into DNA during DNA synthesis (17). Thus, whereas both are markers of cellular proliferation, only BrdU is a specific marker for the S phase. At baseline, the number of BrdU positive hepatocytes was similar in GNMT-KO mice that in WT animals, whereas PCNA staining was higher in the mutant mice (Fig. 2). Following PH, the number

of BrdU and PCNA positive cells increased similarly in the controls and in GNMT-KO mice (Fig. 2). These results indicate, that the increased mortality in GNMT-KO mice after PH is not due to an inhibition of DNA synthesis but probably to increased liver apoptosis.

The LKB1/AMPK/eNOS pathway is inhibited during liver regeneration in GNMT-KO mice

We have previously demonstrated that GNMT-KO mice develop liver steatosis at 3 months of age and multifocal HCC at 8 months of age (5). We have also shown that loss of GNMT induces aberrant methylation of DNA and histones resulting in epigenetic modulation of critical carcinogenesis pathways (5). Consistently, at baseline the phosphorylation of STAT3 and the levels of cyclin D1 and cyclin A were increased in livers from 3-month old GNMT-KO mice as compared to WT animals (Fig. 3a). Following PH, STAT3 phosphorylation fell drastically and the proliferation proteins cyclin D1 and cyclin A remained unchanged in GNMT-KO mice (Fig. 3a,b). As expected, STAT3 phosphorylation, cyclin D1 and cyclin protein content increased in WT animals following PH (Fig. 3a,b). Cyclin E protein levels increased in GNMT-KO mice following PH, although did not reach the same high levels that in control animals (Fig. 3b). The level of p27 protein, an inhibitor of cyclin A, decreased in WT mice but increased in GNMT-KO animals following PH (Fig. 3b). These results, together with the ability of GNMT-KO mice hepatocytes to stimulate DNA synthesis, suggest these hepatocytes are not arrested in the pre-replicative G_1 phase of the cell cycle following PH but progress into the S phase.

AMPK is a critical regulator of liver carbohydrate and fat metabolism that is activated in response to energy stress conditions that elevate intracellular AMP to maintain normal ATP levels (18). There are several reports indicating that the tumor suppressor LKB1 is the upstream activating kinase for the stress responsive AMPK (19). Recently, we have demonstrated that AMPK is activated during liver regeneration via HGF-mediated LKB1 phosphorylation (11), which provides a link between cellular metabolism and cell proliferation. We have also shown that SAMe treatment prior PH prevents HGF-mediated LKB1 and AMPK activation (11). Accordingly, we next determined the phosphorylation of LKB1 and AMPK after PH in GNMT-KO mice and control animals. We found that at baseline both LKB1 and AMPK phosphorylation was reduced in GNMT-KO mice as compared to WT animals (Fig. 4a). We also found that hepatic LKB1 and AMPK are both activated 0.5 hr after PH in WT mice but not in GNMT-KO animals (Fig. 4a). This agrees with the observation that hepatic SAMe content is about 50-fold higher in GNMT-KO mice than in controls (4), and with the present finding showing that whereas in WT mice, as expected (8), liver SAMe content decreased about half following PH, in knockout animals SAMe content remained constant (Table 1).

We have shown that, upon HGF treatment, WT mouse hepatocytes showed an increased phosphorylation of LKB1 and AMPK and that this process is inhibited by the addition of SAMe (10,11). This mechanism would not work in GNMT-KO mice because high hepatic SAMe will prevent HGF-mediated LKB1 and AMPK phosphorylation. To examine this, we measured LKB1 and AMPK phosphorylation after HGF addition in hepatocytes isolated from GNMT-KO mice. In the knockout hepatocytes, HGF failed to induce the phosphorylation of LKB1 and AMPK (Supplementary Fig. 1).

In addition to function as an energy sensor, to provide metabolic adaptation under conditions of energy stress and prepare cells for unfavorable growth conditions, hepatic AMPK regulates also eNOS phosphorylation, a key step for the activation of iNOS and NO synthesis in the liver (11,20), as well as the translocation from the nucleus to the cytoplasm of HuR, an RNA binding protein that increases the half-life of target mRNAs such as iNOS, cyclin A2 and cyclin D1 (10,21). We found that at baseline eNOS phosphorylation, but not cytoplasmic HuR, was reduced in GNMT-KO mice as compared to WT animals (Fig. 4a,b).

We also found that hepatic eNOS phosphorylation and cytoplasmic HuR translocation are activated after PH in WT mice but not in GNMT-KO animals (Fig. 4a,b). The inability of the GNMT-KO hepatocytes to activate AMPK, suggests these hepatocytes have an abnormal metabolic adaptation as well as an anomalous regulation of HuR target genes following PH.

Since GNMT-KO mice show at baseline steatosis and hypermethylation of multiple genes (5), it is possible that impaired liver regeneration may be partially due to these abnormalities. Due to this limitation, we analyzed the effect of GNMT knockdown on HGF-induced cyclin D1 expression in isolated rat hepatocytes. Compared with control cells, hepatocytes transfected with GNMT-specific RNA interference (RNAi) showed a marked decrease in GNMT mRNA without significantly affecting MAT1A expression (Supplementary Fig. 2). As shown also in the graph, hepatocytes transfected with GNMT-specific RNAi reduced cyclin D1 expression in response to HGF stimulation by about 60% compared with control cells. We next used RNAi to silence GNMT *in vivo* in WT mice and to examine the effect of GNMT knockdown on liver regeneration after PH. As seen in Supplementary Fig. 3, mice treated with GNMT-specific RNAi showed a 2-fold reduction in hepatic GNMT mRNA and protein as compared to control mice. As seen also in the figure, following PH mice treated with GNMT-specific RNAi had a marked reduction in hepatic cyclin D1 and A expression as well as in cytoplasmic HuR accumulation compared to control animals. This situation resembles that found in GNMT-KO mice where cyclin D1 and A expression and cytoplasmic HuR content remained unchanged following PH (Fig. 3 and Fig. 4) supporting the concept that GNMT plays an important role in hepatocyte growth during liver regeneration after PH.

Inhibition of AMPK induces NFκB activation in hepatocytes

Given that NFκB activation and the induction of iNOS expression play an important role in liver regeneration (12,13), we determined these two parameters in knockout mice and control animals following PH. At baseline, liver NFκB activation, as evidenced by the nuclear accumulation of total and Ser(536) phosphorylated p65, was higher in GNMT-KO mice than in WT (Fig. 5a). However, 30 min after PH this situation changed drastically, and whereas in WT mice the nuclear content of p65, as expected, markedly increased, in GNMT-KO mice the nuclear content of p65 remained constant and below the levels reached in WT animals (Fig. 5a). Consistent with this abnormal pattern of NFκB signaling is the observation that the expression of iNOS, a NFκB target, was significantly higher in GNMT-KO mice that in WT animals before PH, but whereas the expression of iNOS, as expected (12,13), increased markedly in WT mice following PH, in GNMT-KO mice iNOS expression decreased after PH (Fig. 5b).

Since we found that in GNMT-KO mice liver AMPK phosphorylation is inhibited and NFκB activated, the next question we addressed was if both processes might be related. To this end, we analyzed the phosphorylation of AMPK and the activation of NFκB in hepatocytes isolated from WT mice that were incubated with compound C (CC, a specific inhibitor of AMPK) (16). As shown in Fig. 6a, treatment of hepatocytes with CC inhibited AMPK phosphorylation, increased the phosphorylation and degradation of cytoplasmic IκBα, and induced the translocation and phosphorylation of p65 from the cytosol to the nucleus. Moreover, the addition of CC to WT hepatocytes induced the cleavage of PARP (Fig. 6a). Pretreatment of the hepatocytes with CC for 2 hours prevented further activation of NFκB in response to TNFα (Fig. 6b), and blocked TNFα-induced iNOS expression (Fig. 6c). These experiments reveal a previously unexpected relationship between AMPK phosphorylation, NFκB activation and PARP cleavage.

DISCUSSION

Adult hepatocytes are normally quiescent (in G_0 phase), but have a great replicative capacity and are capable of repopulating the liver when a defect in hepatic mass occurs, such as after PH (12,13). Many studies have emphasized the importance of the activation of the Ras/ERK/MAPK pathway in HGF-induced hepatocyte proliferation and liver regeneration after PH (12,13). Recently, we have uncovered an LKB1/AMPK/eNOS cascade downstream the HGF/MET receptor, that functions also as a critical determinant of hepatocyte proliferation during liver regeneration after PH (11). We have shown that down-regulation of this alternative pathway, using interference RNA, diminishes the mitogenic effect of HGF in hepatocytes (11). A potential mechanism for this is the ability of AMPK to activate the translocation of HuR from the nucleus to the cytoplasm (10). HuR is an RNA binding protein that stabilizes the half-life of a variety of target mRNAs involved in cell-cycle progression, such as cyclin A and cyclin D1, as well as of other mRNAs that play a critical role in liver regeneration after PH, such as iNOS (21). NO synthesis plays an important role in liver regeneration (12,13). Mice lacking either iNOS or eNOS have abnormal liver regeneration after PH (11,22). An additional mechanism by which AMPK regulates hepatocyte proliferation during liver regeneration may be through its capacity to stimulate eNOS phosphorylation and NO production (11,20). Furthermore, AMPK provides a link between cellular metabolism and hepatocyte proliferation during liver regeneration.

In rodents, an early event after PH that precedes DNA synthesis is a fall in hepatic SAMe content (8,11), which is caused by the inactivation of MATI/III induced by the NO generated during liver regeneration (23). This fall in hepatic SAMe content releases the inhibitory effect this molecule exerts on the activation by HGF of the LKB1/AMPK/eNOS cascade (10,11) and, consequently, on the mitogenic effect of HGF (9–11). This mechanism does not work in the MAT1A-KO mouse, because these mice have reduced hepatic SAMe content (3) and MATII is not subject to inactivation by NO (24). Consequently, MAT1A-KO mice exhibit an enhanced activation of the LKB1/AMPK/eNOS cascade (11), which results in loss of responsive to mitogenic signals, impaired regenerative response after PH, increased hepatic growth and the spontaneous development of HCC (7,11,25). Consistently with these findings we have hypothesized that, in the GNMT-KO mouse, the chronic increase in hepatic SAMe content will prevent the activation of the LKB1/AMPK/eNOS cascade following PH and that this will lead to an impaired regenerative response.

Here we demonstrate that DNA synthesis, as determined by the number of BrdU and PCNA positive hepatocytes, appeared comparable between WT and knockout mice after PH, suggesting that GNMT-KO hepatocytes progress normally into the S phase of the cell cycle. This agrees with the observation that upstream signaling pathways required for the G_1/S transition, such as cyclin D1 and cyclin A, are activated in knockout mice both at baseline and following PH. In spite of having a normal DNA synthesis, GNMT-KO mice exhibited an impaired regenerative response following PH. This is documented by a nearly 40% mortality within 48 hours following PH and by the observation that at baseline and during liver regeneration PARP is markedly activated in GNMT-KO mice. The observation that, following PH, multiple pathways playing a critical role in liver regeneration, such as the LKB1/AMPK/eNOS cascade, the cytoplasmic translocation of HuR, the nuclear translocation of NFκB, STAT3 phosphorylation and iNOS expression are not activated following PH, further support the conclusion that liver regeneration is impaired in GNMT-KO mice.

We have previously shown that, after PH, DNA synthesis is impaired in WT mice treated with SAMe (11), and that the mitogenic effect of HGF in isolated hepatocytes is prevented by the addition of this molecule (9). These results contrast with the present observation

showing that DNA synthesis is stimulated in GNMT-KO liver following PH. An explanation for this difference is (Fig. 7), that whereas in SAMe-treated mice liver SAMe content increases transiently about 2-fold (11) in GNMT-KO animals hepatic SAMe content is chronically about 50-fold higher that in WT mice (4). We have previously demonstrated (5) that, as a consequence of this supra-physiological SAMe levels, in GNMT-KO mice liver the expression of Ras and JAK/STAT inhibitors (such as RASSF1, RASSF4, SOCS1-3 and CIS) is suppressed due to promoter methylation and hypermethylation of the histones associated to these tumor suppressor genes, leading to the activation of the Ras and JAK/STAT pathways and facilitating DNA synthesis following PH. However, the activation of the LKB1/AMPK/eNOS cascade following PH is blocked in GNMT-KO mice resulting in impaired liver regeneration. On the contrary, in SAMe-treated mice the fall in hepatic SAMe content and the activation of the LKB1/AMPK/eNOS cascade after PH are prevented but without inducing the activation of the Ras and JAK/STAT pathways (Varela-Rey M, Martínez-Chantar ML, Mato JM, unpublished data), resulting in the inhibition of DNA synthesis and impaired hepatocyte growth (11).

Finally, we have uncovered a previously unexpected relationship between liver AMPK phosphorylation, NFκB activation and PARP cleavage. We found that inactivation of AMPK-phosphorylation with CC recapitulates the effect of GNMT ablation on basal hepatic NFκB activation and PARP cleavage. Moreover, we also found that inactivation of AMPK with CC inhibits TNFα-induced NFκB activation and iNOS expression. These results suggest, that under physiological conditions basal AMPK activity prevents hepatocytes from spontaneous but not from TNFα-induced NFκB activation and that, in GNMT-KO mice, inactivation of AMPK below this protective level by an excess of SAMe, although leads to NFκB activation and PARP cleavage, renders hepatocytes insensitive to TNFα-induced NFκB activation and iNOS expression.

Our model, however, has some limitations to study the role of GNMT during liver regeneration. Since GNMT-KO mice show at baseline steatosis and hypermethylation of multiple genes (5), it is possible that impaired liver regeneration may be partially due to these abnormalities. Due to this limitation, which is common to many other knockout mouse models used to delineate the importance of the respective gene in liver regeneration, our results will need to be validated with a time-specific GNMT-KO mouse model. However, the finding that hepatocytes transfected with GNMT-specific RNAi had a reduced expression of cyclin D1 in response to HGF together with the observation that GNMT knockdown in WT mice reduced the expression of cyclin D1 and A as well as the accumulation of cytoplasmic HuR after PH supports the hypothesis that GNMT plays an important role in liver regeneration. Moreover, because there are patients with GNMT mutations and have spontaneous liver disease (28,29), studying liver regeneration in the GNMT-KO model is relevant at least with respect to these individuals.

Supplementary Material

Refer to Web version on PubMed Central for supplementary material.

List of abbreviations

AMPK	AMP-activated protein kinase
BrdU	bromo deoxyuridine
CC	compound C
GNMT	glycine *N*-methyltransferase

GNMT-KO	glycine *N*-methyltransferase knockout
HCC	hepatocellular carcinoma
HGF	hepatocyte growth factor
MAT	methionine adenosyltransferase
eNOS	endothelial nitric oxide synthase
iNOS	inducible nitric oxide synthase
PARP	poly (ADP-ribose) polymerase
PH	partial hepatectomy
RNAi	RNA interference
SAMe	*S*-adenosylmethionine

Acknowledgments

We thank Begoña Rodríguez and for technical assistance.

Financial support.

This work is supported by grants from NIH AT-1576 (to S.C.L., M.L.M-C. and J.M.M.), DK15289 (to C.W.), SAF 2008-04800, HEPADIP-EULSHM-CT-205 and ETORTEK-2008 (to J.M.M. and M.L.M.-C); and Fundación “La Caixa” (to M.L.M.-C.). Ciberehd is funded by the Instituto de Salud Carlos III.

REFERENCES

1. Mato JM, Martínez-Chantar ML, Lu SC. Methionine metabolism and liver disease. Ann Rev Nutr. 2008; 28:273–293. [PubMed: 18331185]
2. Kotb M, Mudd SH, Mato JM, Geller AM, Kredich NM, Chou JY, et al. Consensus nomenclature for the mammalian methionine adenosyltransferase genes and gene products. Trends Genet. 1997; 13:51–52. [PubMed: 9055605]
3. Lu SC, Alvarez L, Huang ZZ, Chen L, An W, Corrales FJ, et al. Methionine adenosyltransferase 1A knockout mice are predisposed to liver injury and exhibit increased expression of genes involved in proliferation. Proc Natl Acad Sci USA. 2001; 98:5560–5565. [PubMed: 11320206]
4. Luka Z, Capdevila A, Mato JM, Wagner C. A glycine N-methyltransferase knockout mouse model for humans with deficiency of this enzyme. Transgenic Res. 2006; 15:393–397. [PubMed: 16779654]
5. Martínez-Chantar ML, Vázquez-Chantada M, Ariz U, Martínez N, Varela M, Luka Z, et al. Loss of the glycine N-methyltransferase gene leads to steatosis and hepatocellular carcinoma in mice. Hepatology. 2008; 47:1191–1199. [PubMed: 18318442]
6. Mato JM, Lu SC. Role of S-adenosyl-L-methionine in liver health and injury. Hepatology. 2007; 45:1306–1312. [PubMed: 17464973]
7. Martínez-Chantar ML, Corrales FJ, Martínez-Cruz LA, García-Trevijano ER, Huang ZZ, Chen L, et al. Spontaneous oxidative stress and liver tumors in mice lacking methionine adenosyltransferase 1A. FASEB J. 2002; 16:1292–1294. [PubMed: 12060674]
8. Huang ZZ, Mao Z, Cai J, Lu SC. Changes in methionine adenosyltransferase during liver regeneration in the rat. Am. J. Physiol. 1998; 38:G14–G21. [PubMed: 9655679]
9. García-Trevijano ER, Martínez-Chantar ML, Latasa MU, Mato JM, Avila MA. NO sensitizes rat hepatocytes to proliferation by modifying S-adenosylmethionine levels. Gastroenterology. 2002; 122:1355–1363. [PubMed: 11984522]
10. Martínez-Chantar ML, Vázquez-Chantada M, Garnacho M, Latasa MU, Varela-Rey M, Dotor J, et al. S-Adenosylmethionine regulates cytoplasmic HuR via AMPK-activated kinase. Gastroenterology. 2006; 131:223–232. [PubMed: 16831604]

11. Vázquez-Chantada M, Ariz U, Varela-Rey M, Embade N, Martínez N, Fernández D, et al. Evidence for an LKB1/AMPK/eNOS cascade regulated by HGF, S-adenosymehtionine and NO in hepatocyte proliferation. Hepatology. 2009; 49:608–617. [PubMed: 19177591]
12. Fausto N, Campbell JS, Riehle KJ. Liver regeneration. Hepatology. 2006; 43:S45–S53. [PubMed: 16447274]
13. Michalopoulos GM. Liver regeneration. J Cell Physiol. 2007; 213:286–300. [PubMed: 17559071]
14. Higgins BC, Andersen RM. Experimental pathology of liver: restoration of liver of the white rat following partial surgical removal. Arch Pathol. 1931; 12:186–202.
15. Leffert HL, Koch KS, Moran T, Williams M. Liver cells. Methods Enzymol. 1979; 58:536–544. [PubMed: 423789]
16. Rencurel F, Foretz M, Kaufmann MR, Strocka D, Looser R, Leclerc I, et al. Stimulation of AMP-activated protein kinase is essential for the induction of drug metabolizing enzymes by Phenobarbital in human and mouse liver. Mol Pharmacol. 2006; 70:1925–1934. [PubMed: 16988011]
17. Assy N, Minuk GY. Liver regeneration: methods for monitoring and their applications. J. Hepatol. 1997; 26:945–952. [PubMed: 9126813]
18. Hardie DG, Hawley SA, Scott JW. AMP-activated protein kinase-development of the energy sensory concept. J Physiol. 2006; 574:7–15. [PubMed: 16644800]
19. Hawley SA, Boudeau J, Reid JL, Mustard KJ, Udd L, Makela TP, et al. Complexes between the LKB1 tumor suppressor, STRADα/β, are upstream kinases in the AMP-activated protein kinase cascade. J Biol. 2003; 2:28. [PubMed: 14511394]
20. Gobeil F, Zhu T, Brault S, Geha A, Vazquez-Tello A, Fortier A, et al. Nitric oxide signaling via nuclearized endothelial nitric-oxide synthase expression of the immediate early genes iNOS and mPGES-1. J Biol Chem. 2006; 281:16058–16067. [PubMed: 16574649]
21. Wang W, Craig M, Caldwell SL, Furneaux H, Gorospe M. HuR regulates cyclin A and cyclin B1 mRNA stability during cell proliferation. EMBO J. 2000; 19:2340–2350. [PubMed: 10811625]
22. Rai RM, Lee FY, Rosen A, Tang SQ, Lin HZ, Koteish A, et al. Impaired liver regeneration in inducible nitric oxide synthase deficient mice. Proc Natl Acad Sci USA. 1998; 95:1329–1334.
23. Ruiz F, Corrales FJ, Miqueo C, Mato JM. Nitric oxide inactivates rat hepatic methionine adenosyltransferase in vivo by S-nitrosylation. Hepatology. 1998; 28:1051–1057. [PubMed: 9755242]
24. Mato JM, Corrales FJ, Lu SC, Avila MA. S-Adenosylmethionine: a control switch that regulates liver function. FASEB J. 2002; 16:15–26. [PubMed: 11772932]
25. Chen L, Zeng Y, Yang H, Lee TD, French SW, Corrales FJ, et al. Impaired liver regeneration in mice lacking methionine adenosyltranferase 1A. FASEB J. 2004; 18:914–916. [PubMed: 15033934]
26. Tseng TL, Shih YP, Huang YC, Wang CW, Chen PH, Chang JG. Genotypic and phenotypic characterization of a putative tumor susceptibility gene, GNMT, in liver cancer. Cancer Res. 2003; 63:647–654. [PubMed: 12566309]
27. Avila MA, Berasain C, Torres L, Martínez-Duce A, Corrales FJ, Yang H, et al. Reduced mRNA abundance of the ain enzymes involved in methionine metabolism in human liver cirrhosis and hepatocellular carcinoma. J Hepatol. 2000; 33:907–914. [PubMed: 11131452]
28. Mudd SH, Cerone R, Schiaffino MC, Fantasia AR, Minniti GU, Caruso U, et al. Glycine N-methyltransferase deficiency: a novel inborn error causing persistent isolated hypermethioninaemia. J Inherit Metab Dis. 2001; 24:448–464. [PubMed: 11596649]
29. Augoustides-Savvopoulou P, Luka ZS, Karyda S, Stabler SP, Allen RH, Patsiaoura K, et al. Glycine N-methyltransferase defieciency: a new patient with a novel mutation. J Inherit Metab Dis. 2003; 26:745–749. [PubMed: 14739680]
30. Gil B, Pajares MA, Mato JM, Alvarez L. Glucocorticoid regulation of hepatic S-adenosylmethionine synthetase gene expression. Endocrinology. 1997; 138:1251–1258. [PubMed: 9048633]

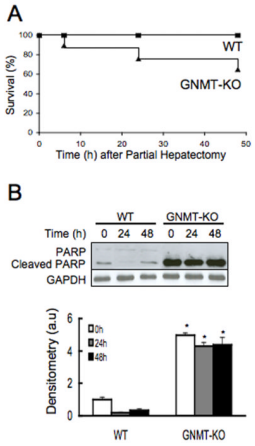

Figure 1.

Mortality and PARP activation in WT and GNMT-KO mice after PH. (A) Cumulative survival of the WT (n = 37) and GNMT-KO (n = 31) mice after PH. The difference between the groups was statistically significant ($P < 0.05$). (B) PARP cleavage in WT and GNMT-KO after PH. Top: Liver samples from WT and GNMT-KO mice were obtained at 0, 24 and 48 hours after PH and analyzed (30 μg/lane) via Western blotting with the indicated antibodies. Data are representative of an experiment performed five times. Bottom: A graphical representation (mean ± SEM) of the densitometry changes of PARP cleavage, in liver samples obtained at 0, 24 and 48 hours after PH from WT and GNMT-KO mice, is shown. *, $P < 0.05$ GNMT-KO vs. WT mice at the same time point, n = 5.

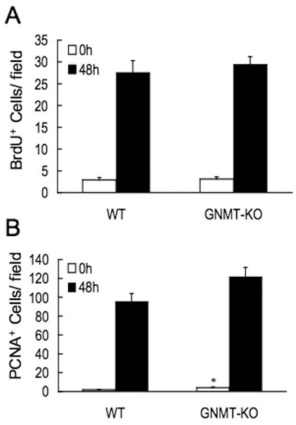

Figure 2.

Hepatocyte proliferation after PH as assessed by BrdU and PCNA incorporation. (A) The number of BrdU-positive cells at 0 hours and 48 hours after PH were counted and expressed as the number of positive cells per field in liver specimens from WT and GNMT-KO mice. (B) The number of PCNA-positive cells at 0 hours and 48 hours after PH were counted and expressed as the number of positive cells per field in liver specimens from WT and GNMT-KO mice. In both cases, the number of positive cells was counted in 10 microscope fields using a 40× objective and a 10× eyepiece with a Zeiss AX10 microscope. Data (mean ± SEM) are the average of five experiments performed independently. *, $P < 0.05$ GNMT-KO vs. WT mice at the same time point.

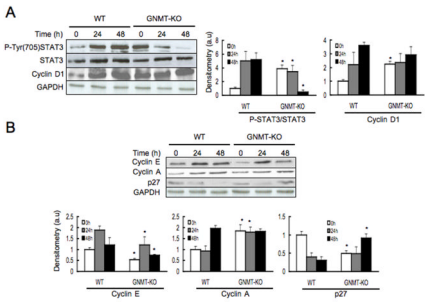

Figure 3.

Phosphorylation of STAT3 and protein expression of cyclin D1, cyclin E, cyclin A and p27, in WT and GNMT-KO mice following PH. (A) Left: Liver samples from WT and GNMT-KO mice were obtained at 0, 24 and 48 hours after PH and analyzed (30 μg/lane) via Western blotting with the indicated antibodies. Data are representative of an experiment performed five times. Right: A graphical representation (mean ± SEM) of the densitometry changes of STAT3 phosphorylation and cyclin D1 protein content, in liver samples from WT and GNMT-KO mice after PH, is shown. (B) Top: liver samples from WT and GNMT-KO mice were obtained at 0, 24 and 48 hours after PH and analyzed (30 μg/lane) via Western blotting with the indicated antibodies. Data are representative of an experiment performed five times. Bottom: A graphical representation (mean ± SEM) of the densitometry changes of cyclin E, cyclin A and p27 protein content, in liver samples from WT and GNMT-KO mice after PH, is shown. *, $P < 0.05$ GNMT-KO vs. WT mice at the same time point, n = 5.

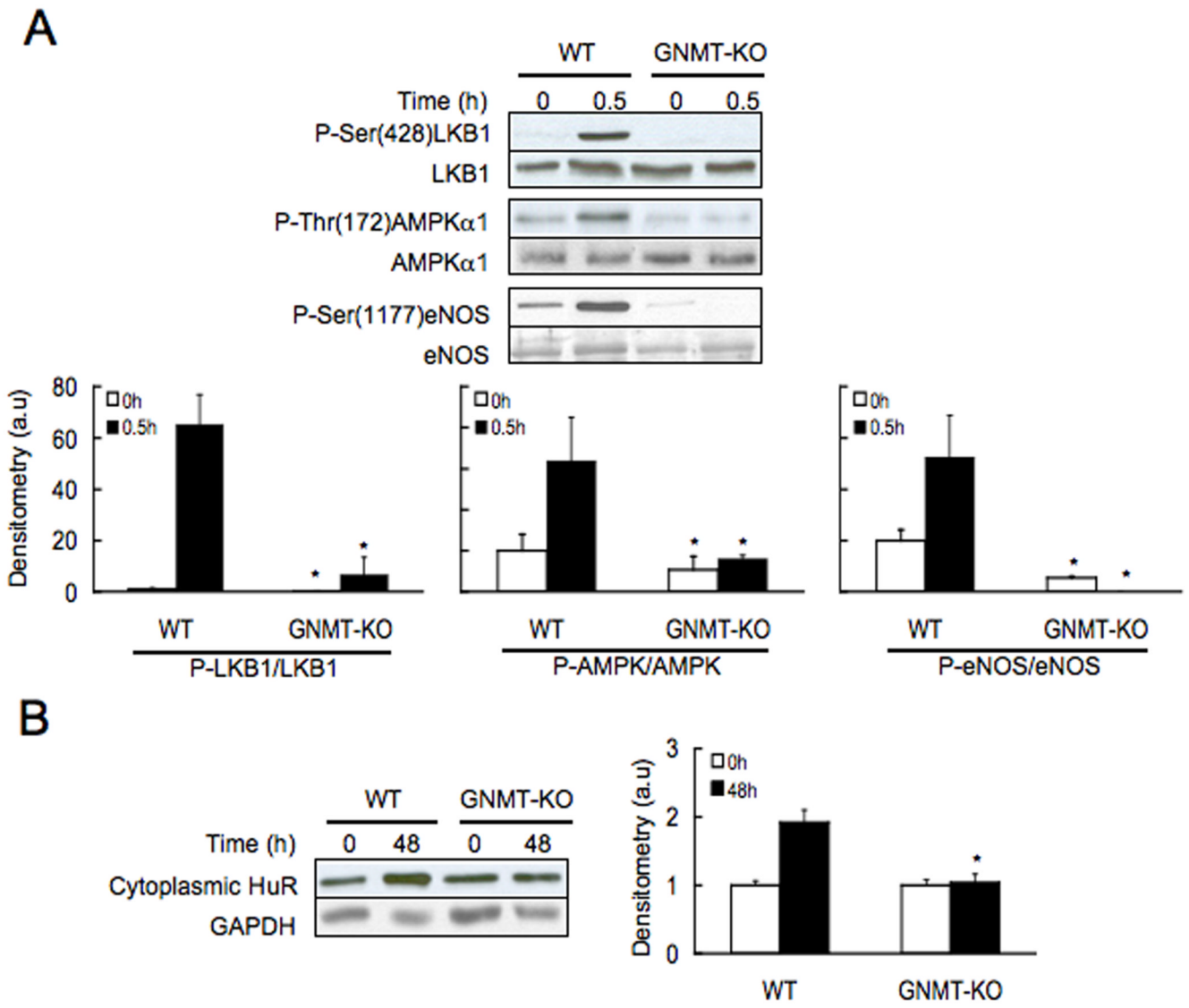

Figure 4.

Phosphorylation of LKB1, AMPK and eNOS, and cytoplasmic HuR content in WT and GNMT-KO mice during liver regeneration after PH. (A) Top: Liver samples were obtained before and 30 minutes after PH and analyzed (30 μg/lane) via Western blotting with the indicated antibodies. Data are representative of an experiment performed five times. Bottom: A graphical representation (mean ± SEM) of the densitometry changes of LKB1, AMPK and eNOS phosphorylation, in liver samples from WT and GNMT-KO mice after PH, is shown. (B) Left: Liver samples were obtained before and 48 hours after PH and analyzed (30 μg/lane) via Western blotting with the indicated antibodies. Data are representative of an experiment performed five times. Right: A graphical representation (mean ± SEM) of the densitometry changes of cytoplasmic HuR protein levels, in liver samples from WT and GNMT-KO mice after PH, is shown. *, $P < 0.05$ GNMT-KO vs. WT mice at the same time point, n = 5.

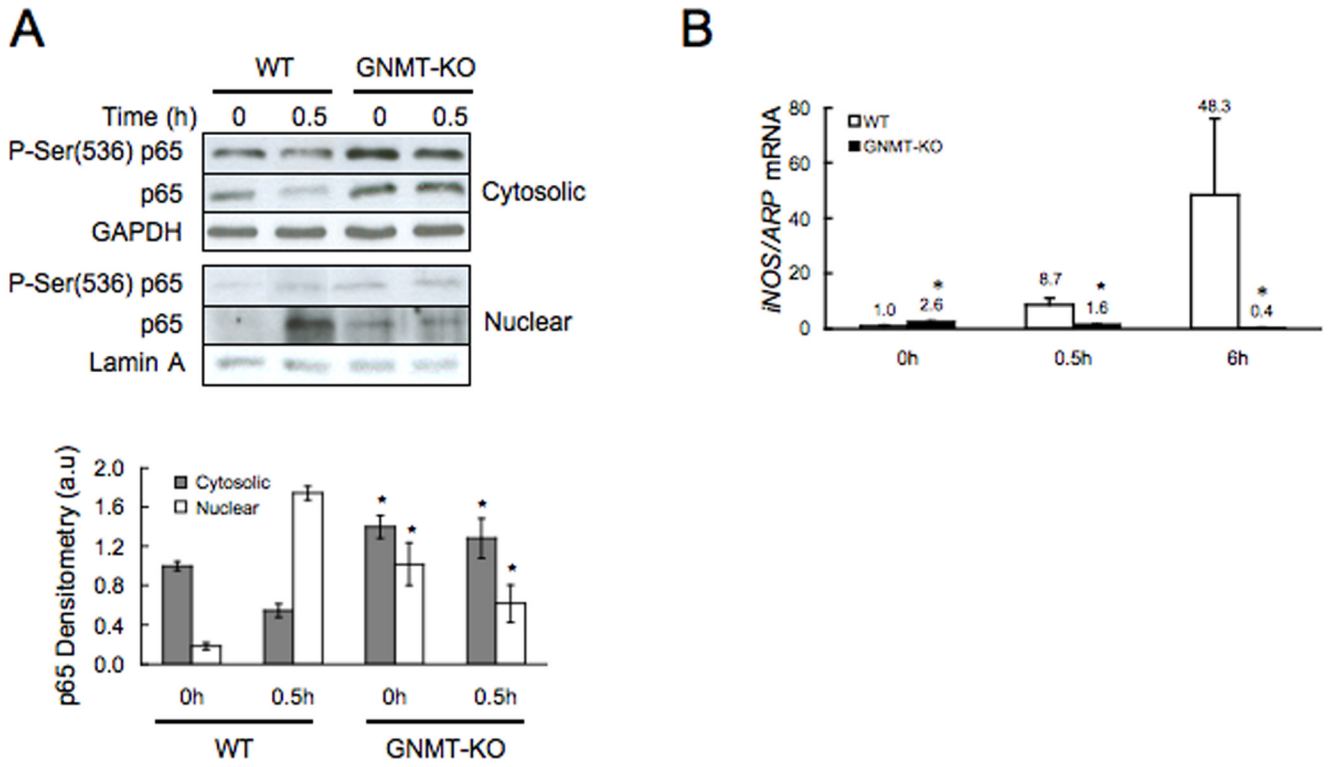

Figure 5.

Western blot analysis of cytosolic and nuclear p65 and real time PCR of iNOS in WT and GNMT-KO mice during liver regeneration after PH. (A) Top: Cytosolic and nuclear liver samples were obtained before and 30 minutes after PH and analyzed (30 μg/lane) via Western blotting with the indicated antibodies. Data are representative of an experiment performed five times. Bottom: A graphical representation (mean ± SEM) of the densitometry changes of cytosolic and nuclear p65, in liver samples from WT and GNMT-KO mice after PH, is shown. (B) Liver samples were obtained before, 30 minutes and 6 hours after PH and iNOS mRNA levels analyzed via RT-PCR. Data (mean ± SEM) are the average of five experiments in triplicate performed independently. *, $P < 0.05$ GNMT-KO vs. WT mice at the same time point. Numbers on top of the bars indicate the precise value of each measurement.

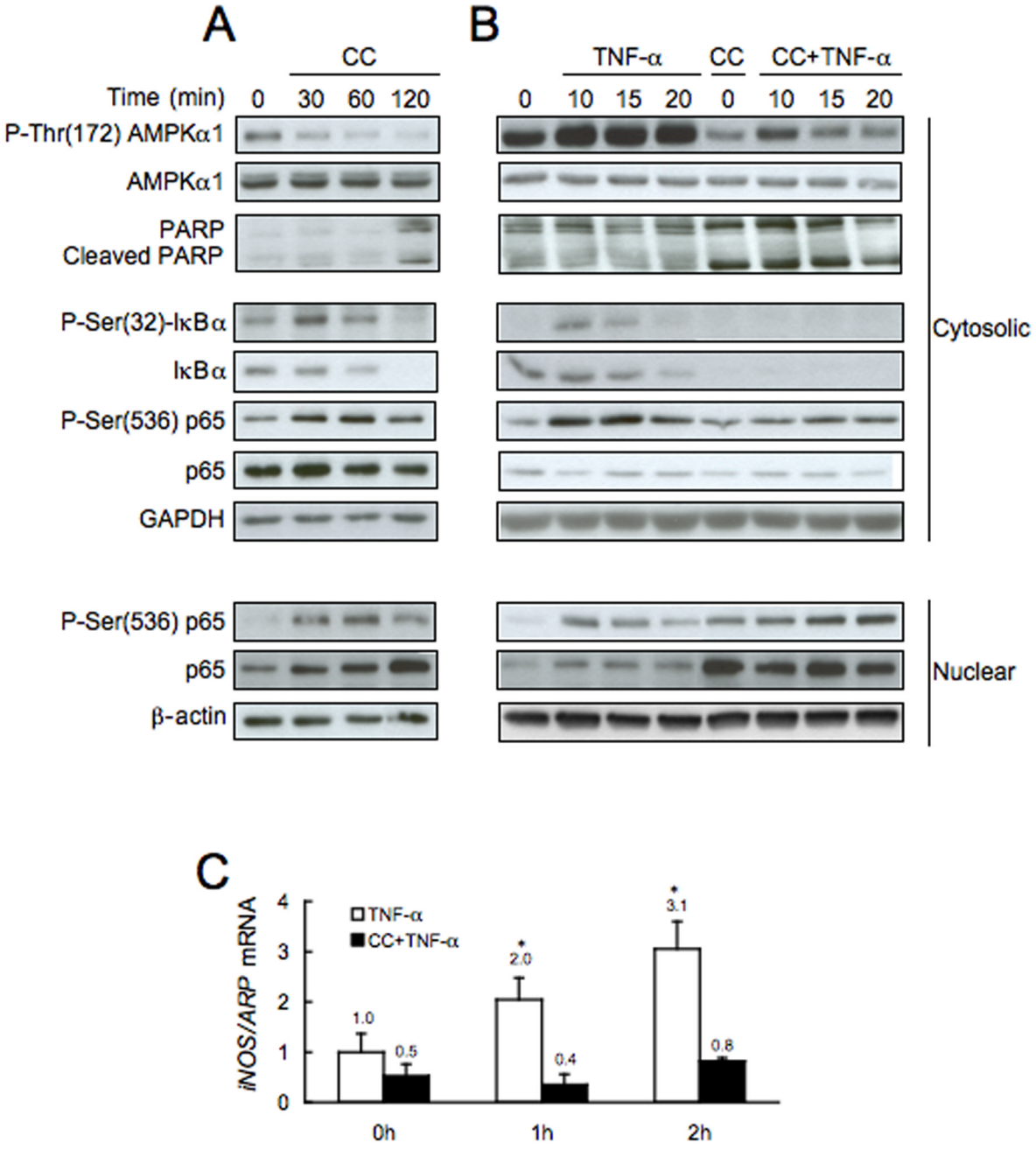

Figure 6.

Effect of compound C (CC) on basal and TNF-α induced AMPK phosphorylation, NFκB activation and iNOS expression in isolated mouse hepatocytes. (A) Phosphorylation of AMPK, PARP cleavage, and activation of NFκB, by removal of the inhibitory IκBα through phosphorylation and translocation of p65 to the nucleus, was analyzed (30 μg/lane), via Western blotting with the indicated antibodies, in isolated hepatocytes before, 30, 60 and 120 minutes after the addition of CC (40 μM). (B) Phosphorylation of AMPK, PARP cleavage, and activation of NFκB, by removal of the inhibitory IκBα through phosphorylation and translocation of p65 to the nucleus, was analyzed (30 μg/lane), via Western blotting with the indicated antibodies, in isolated hepatocytes before, 10, 15 and 20

minutes after the addition of TNF-α (10 ng/ml). Hepatocytes were incubated in the presence or absence of CC (40 μM) during 120 minutes prior the addition of TNF-α. Results are representative of four independent experiments. (C) iNOS expression was analyzed by RT-PCR in isolated hepatocytes incubated in the presence or absence of CC (40 μM) during 120 minutes prior the addition of TNF-α (10 ng/ml). Data (mean ± SEM) are the average of four experiments in triplicate performed independently.

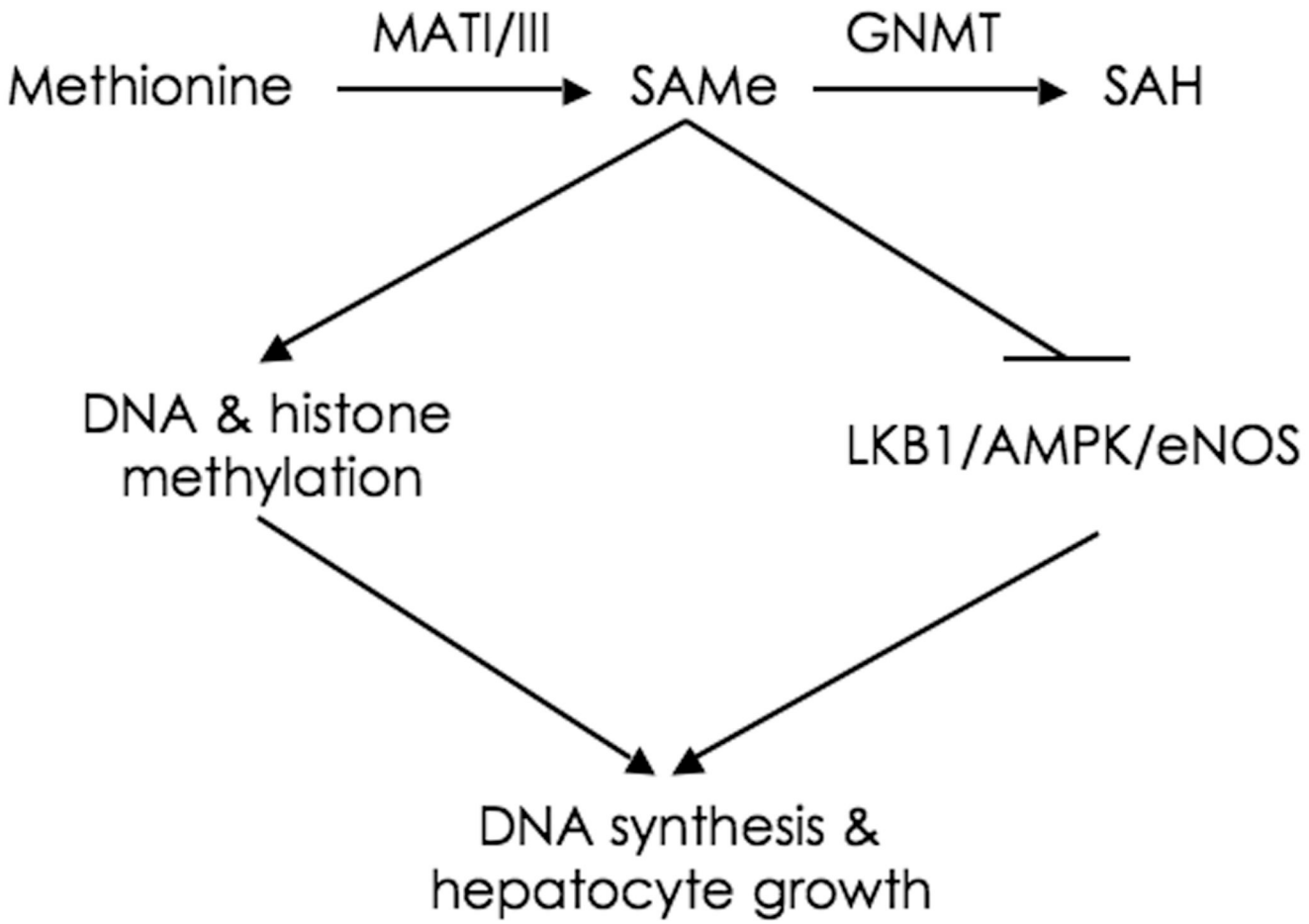

Figure 7.

MATI/III and GNMT control DNA synthesis and hepatocyte growth. Hepatic SAMe content is maintained constant by the combined action of MATI/III and GNMT. SAMe induces DNA and histone methylation as well as the inactivation of the LKB1/AMPK/eNOS pathway. Under normal conditions, liver SAMe content is low enough not to induce spontaneous DNA and histone hyper-methylation resulting in epigenetic modulation of critical carcinogenesis pathways, such as the Ras and JAK/STAT pathways, but is sufficiently elevated to avoid the spontaneous activation of the LKB1/AMPK/eNOS cascade resulting in uncontrolled DNA synthesis and hepatocyte growth. During liver regeneration following PH, SAMe content transiently decreases releasing its inhibitory effect on the LKB1/AMPK/eNOS cascade, which contributes to normal DNA synthesis and hepatocyte proliferation. In MATI/III deficient mice, SAMe content is chronically reduced resulting in the activation of the LKB1/AMPK/eNOS cascade, increased DNA synthesis and hepatocyte growth, and impaired liver regeneration after PH. In SAMe-treated mice, the fall in hepatic SAMe content and the activation of the LKB1/AMPK/eNOS cascade following PH are prevented but without inducing DNA and histone hyper-methylation, resulting in the inhibition of DNA synthesis and impaired hepatocyte growth. In GNMT deficient mice, SAMe content is chronically about 50-fold higher that in WT animals resulting in inhibition of the LKB1/AMPK/eNOS cascade. We have previously demonstrated (5), that in GNMT-KO mice liver DNA and histones are hyper-methylated leading to the activation of the Ras and JAK/STAT pathways. After PH, activation of the Ras and JAK/STAT cascades

facilitates DNA synthesis and hepatocyte growth although the inhibition of multiple pathways playing a critical role in liver regeneration, such as the activation of the LKB1/AMPK/eNOS cascade, the cytoplasmic translocation of HuR, iNOS activation, and STAT3 phosphorylation, impair this process. SAH, S-adenosylhomocysteine.

Table 1

Hepatic SAMe content in wild type (WT) and GNMT-KO mice before and 48 hours after partial hepatectomy.

SAMe nmol/mg protein	0 hours	48 hours
WT	0.47 ± 0.03	0.25 ± 0.03*
GNMT-KO	21.73 ± 0.88	20.64 ± 0.97

Liver samples were obtained before (0 hours) and 48 hours after PH and the content of SAMe determined.

*$P<0.05$, 48 hours vs. 0 hours [n = 5].